Applied Catalysis A: General 478 (2014) 1–8

Contents lists available at ScienceDirect

Applied Catalysis A: General

journal homepage: www.elsevier.com/locate/apcata

Carbon nanotubes as catalyst for the aerobic oxidation of cumene to cumene hydroperoxide

Shixia Liao, Feng Peng*, Hao Yu, Hongjuan Wang

School of Chemistry and Chemical Engineering, South China University of Technology, Guangzhou, Guangdong 510640, China

ARTICLE INFO

Article history:
Received 12 December 2013
Received in revised form 19 February 2014
Accepted 10 March 2014
Available online 27 March 2014

Keywords:
Cumene
Catalytic oxidation
Carbon nanotubes
Cumene hydroperoxide

ABSTRACT

The effective oxidation reaction system using the commercial carbon nanotubes (CNTs) as catalysts for the liquid aerobic oxidation of cumene to cumene hydroperoxide (CHP) under low temperature is reported in this paper. Several reaction parameters, including the temperature, catalyst content, oxygen flow rate and reaction time were carefully studied. Under optimal conditions, cumene conversion of 24.1% with CHP selectivity of 88.4%, close to that of metal catalyst, was obtained. Cumene oxidation catalyzed by CNTs was proved a radical-involved reaction, and the outstanding catalytic performance was attributed to CHP decomposition catalyzed by CNTs to produce free radicals. Oxygenated functional groups on the surface of catalyst showed a negative effect on cumene oxidation due to the localization of electrons after the introducing of defects and oxygenated functional groups. CNTs as catalysts also showed desirable recyclability after five cycling tests. This study not only provides an applicable method for selective oxidation of cumene to CHP, but also gives some useful information on catalytic role of CNTs-catalyzed liquid-phase oxidation reactions of aromatic hydrocarbons.

1. Introduction

Liquid-phase oxidation of hydrocarbons with air or molecular oxygen to high value-added oxygen-containing compounds such as peroxides, alcohols, ketones and carboxylic acids is a significant and efficient petro-chemical industrial process [1]. Liquid aerobic oxidation of cumene to cumene hydroperoxide (CHP) is one of such reactions. CHP is an important intermediate in the three-step cumene-phenol process which starts with the alkylation of benzene with propylene to produce cumene, continues with the oxidation of cumene to CHP, and ultimately produces phenol and acetone by the decomposition of CHP in acid medium [2]. Today, more than 90% of the phenol in the world is produced by this route. In the conventional cumene oxidation process, air was used as oxidant and CHP was used as initiator under high temperature and pressure, and alkaline solution was used to instantaneously neutralize the acids produced [3]. Except low efficiency, there are still some drawbacks such as poor safety, difficult catalyst recycling, and negative environmental impact. With the increased awareness of green chemistry and the development of phenol chemical industry, much attention has been paid on the research of new catalyst system. A lot of common-used transition metal catalysts, such as Cu(I)/Cu(II), Co(II)/(III) and Mn(II)/(III), whether as oxides [4,5], complexes [6,7], or supported catalysts [8] have been typically investigated in the oxidation process experimentally. However, none of these catalysts have been applied in industry. Consequently, it is necessary to develop more efficient, environment-friendly, easily-separated and easily-industrialized catalysts in cumene oxidation process.

Among the many attempts to find feasible catalysts for cumene oxidation, it is particularly interesting to note that nano-sized carbon materials have attracted much attention, owing to their physicochemical and mechanical property, such as high surface areas, outstanding electron conductivity, corrosion resistance, and thermal stability [9–11]. In addition, from an environmental point of view, carbon materials enable a clean disposal by combustion after a certain life-time, making them attractive alternatives to conventional metal oxide catalysts for a more sustainable petrochemical production process. Recently, carbon nanotubes have been directly applied as catalysts in the oxidative dehydrogenation (ODH) reactions of alkanes to corresponding alkenes [12–14], catalytic wet air oxidation (CWAO) [15–17], and oxidation of aldehydes [18] and so on. Their excellent catalytic performance has been thought to be relevant to their microstructure and surface functionalities. For example, in the most prominent and high-industrial-relevance ODH reaction, the widely-accepted reaction mechanism is that rich-in-electron diketone-like carbonyl ($\rangle C{=}O$) groups on the surface of carbon materials are active sites [14]. However, S. Yang found easily-broken carboxylic acid groups on the

---

* Corresponding author. Tel.: +86 20 87114916; fax: +86 20 87114916.
E-mail address: cefpeng@scut.edu.cn (F. Peng).

http://dx.doi.org/10.1016/j.apcata.2014.03.024
0926-860X/

surface of CNTs played an important role in CWAO of phenol [15]. Meanwhile, basis surface was also thought to be responsible for improved catalytic performance in CWAO [16,17]. More recently, carbon materials were found to be active for the direct liquid-phase aerobic oxidation of aromatic hydrocarbon. In our previous work, we proved that pristine carbon nanotubes could directly catalyze the aerobic oxidation of cyclohexane to adipic acid and ethylbenzene to acetophenone, and the surface defects and oxygen functionalities had a negative effect on the activity [19,20]. Jing-He Yang etc. also proved that metal-free graphene-based catalyst was effective for one-step oxidation of benzene to phenol with hydrogen peroxide as the oxidant [21]. However, up to now, it is rarely reported that nanostructured carbon as catalyst for selective oxidation reaction of cumene, and the basic knowledge about carbon catalysis remains limited.

Herein, by using cost-cheap commercial carbon nanotubes as catalyst and oxygen as oxidant, we explored their catalytic activity in the aerobic oxidation of cumene without solvent at atmospheric pressure. The influence of catalyst surface oxygen-containing functional groups on catalytic performance was also discussed. The high reaction activity of cumene oxidation and the recyclability of carbon catalyst make this reaction system attractive for potential industrial application.

2. Experimental

2.1. Preparation of catalysts

The commercial carbon nanotubes (denoted as CNTs, $S_{BET} = 85.3\,m^2\,g^{-1}$, $d = 30–50$ nm) were purchased from Shenzhen Nanotech Port Co. Ltd (NTP). They were stirred to purify in hydrochloric acid or heated to reflux in 9 mol/L HNO_3 for 0.5, 2 and 4 h to introduce oxygen functional groups, then washed with deionized water until pH reached 6–7, and dried in air at 383 K overnight. The obtained materials were denoted as CNTs-HNO_3-0.5, CNTs-HNO_3-2, and CNTs-HNO_3-4, respectively. In addition, CNTs-HNO_3-2 samples were subjected to heat treatment in a horizontal tubular quartz furnace with 4 cm inner diameter under argon atmosphere at 873 K or 1173 K for 2 h and then cooled under argon, denoted as CNTs-HNO_3-2-873 and CNTs-HNO_3-2-1173, respectively [22,23].

2.2. Characterizations

Brunauer-Emmett-Teller (BET) specific surface areas were measured by N_2 adsorption at liquid N_2 temperature in an ASAP 2010 analyzer. Raman spectra were obtained in a LabRAM Aramis micro-Raman spectrometer with an excitation wave-length at 532 nm with 2 μm spot size. TEM (transmission electron microscopy) and HRTEM (high resolution transmission electron microscopy) images were obtained with a FEI Tecnai G2 12 microscope operated at 100 kV and a JEOL JEM2010 microscope operated at 200 kV. Specimens for TEM and HRTEM were prepared by ultrasonically suspending the sample in acetone and depositing a drop of the suspension onto a grid. X-ray photoelectron spectroscopy (XPS) analysis was performed in a Kratos Axis ultra (DLD) spectrometer equipped with an Al Kα X-ray source in ultrahigh vacuum (UHV) ($<10^{-10}$ Torr). The binding energies (±0.2 eV) were referenced to the C1s peak at 284.6 eV. The surfaces of samples were cleaned by heat treatment at 373 K in UHV prior to the measurements.

2.3. Catalytic tests

The liquid oxidation reactions were carried out in a three-necked flask (20 mL), supplied with a magnetic stirrer, reflux condenser and the oil bath. Cumene (10 mL) and catalyst were put into the flask, sonicated for 5 min, and then heated to preconcerted temperature followed by the bubbling of oxygen at a constant flow rate. The main product of cumene oxidation is CHP, the by-products are acetophenone (AP) and 2-benzyl-2-propanol (BP), as shown in Scheme 1. The CHP concentration was determined according to the iodometric method [24]. After the reduction of generated CHP to BP *via* triphenylphosphine reaction [25], the other products in the liquid phase were detected by gas chromatography (an Agilent GC-6820) equipped with a 30 m × 0.25 mm × 0.25 μm HP-5 capillary column and a flame ionization detector (detector temperature 553 K, injector temperature 553 K, and oven temperature 413 K) using toluene as external standard. Cumene conversion (X) and products selectivity (S) were calculated using the following equations (I)–(IV).

$$X = \frac{n_{i,cumene} - n_{f,cumene}}{n_{i,cumene}} \times 100\% \tag{I}$$

$$S_{CHP} = \frac{n_{f,CHP} - n_{i,CHP}}{n_{f,CHP} - n_{i,CHP} + n_{f,BP} + n_{f,AP}} \times 100\% \tag{II}$$

$$S_{BP} = \frac{n_{f,BP}}{n_{f,CHP} - n_{i,BP} + n_{f,BP} + n_{f,AP}} \times 100\% \tag{III}$$

$$S_{AP} = \frac{n_{f,AP}}{n_{f,CHP} - n_{i,CHP} + n_{f,BP} + n_{f,AP}} \times 100\% \tag{IV}$$

where $n_{i,m}$ and $n_{f,m}$, respectively, mean the moles of m in initial reactant and final product.

The thermolysis tests of CHP were conducted according to Ref. [26]. 8 mL acetonitrile and 0.1 g catalyst were added in a flask, sonicated for 5 min and then placed in an oil bath at 353 K. After flushing with N_2 for 5 min, CHP (2 g) was added and the reaction was conducted in a closed system. The unreacted CHP was tested by aforementioned iodometric method.

3. Results and discussion

3.1. The optimization of reaction conditions

Cumene liquid-phase oxidation reaction was operated at atmospheric pressure with oxygen as oxidant with carbon nanotubes as catalyst and no solvent was added. In order to optimize the reaction parameters and provide a basis for further mechanism research, the effects of reaction conditions, including catalyst amount, reaction temperature, oxygen flow rate and reaction time on the catalytic performance were investigated in detail.

The effect of catalyst amount on the catalytic activity of cumene under 353 K was shown in Fig. 1A. The flow rate of O_2 was controlled at 10 cm^3/min. In the absence of catalyst, the autoxidation rate of cumene is very slow (X = 2.7%, 8 h). After the addition of 50 mg CNTs, the conversion of cumene increased to 17.8% with an outstanding selectivity of 90.8% to CHP. With the increase of CNTs content, the conversion of cumene also increased. On the contrary, too much catalyst leads to decline in selectivity to CHP. With 200 mg CNTs, the 35.0% conversion of cumene was obtained, whereas the selectivity to CHP obviously decreased to 76.2%. This indicates that CNTs play an important role in cumene oxidation. To get an acceptable selectivity to CHP, 100 mg CNTs under reaction condition was chosen.

The effect of reaction temperature on the catalytic performance of cumene was shown in Fig. 1B. It revealed that cumene oxidation could be well carried out under a rather low temperature as 343 K. The conversion of cumene increased significantly with the reaction temperature increasing. Under 353 K, the selectivity to CHP remained stable value of 88.4%. When the temperature reached 373 K, the selectivity to CHP dropped dramatically possibly due to the accelerated decomposition of CHP. Thus, the reaction

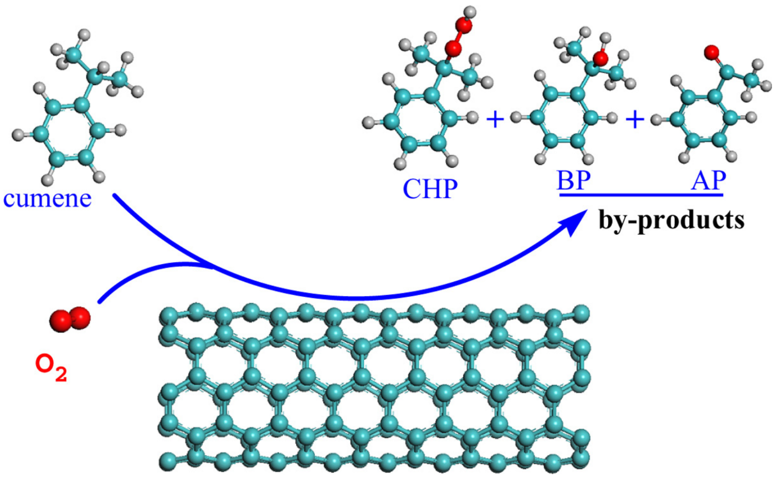

Scheme 1. Oxidation products of cumene on carbon nanotubes.

Table 1
Oxidation of cumene under different catalytic systems[a].

Entry	Catalyst	Conversion (%)	Selectivity (%)		
			AP	BP	CHP
1	CNTs	24.1	1.6	10.0	88.4
2	NaOH[b]	15.1	3.9	8.5	87.6
3	CuO[c]	38.8	5.7	21.1	73.2
4	CuO[d]	31.6	2.7	14.2	83.1

[a] Reaction conditions: cumene 10 mL, catalyst 0.1 g, 353 K, 8 h, O_2 flow rate of 10 cm^3/min.
[b] 10% NaOH aqueous solution with 2% CHP as initiator.
[c] Commercial CuO.
[d] CuO prepared according to Catalyst 2 of Ref. [4].

temperature is an important factor to maintain a high CHP selectivity and a high cumene conversion. For this reason, the proper reaction temperature of 353 K was selected for cumene oxidation to CHP.

Fig. 1C indicates the effect of O_2 flow rate on catalytic performance of cumene. With the increase of oxygen flow rate from 5 cm^3/min to 10 cm^3/min, the conversion of cumene improved slightly while the selectivity to CHP remained almost at the same level. However, further increased oxygen flow rate resulted in the CHP selectivity decreasing. Hence, the flow rate of oxygen was chosen at 10 cm^3/min.

The effect of reaction time on catalytic activity of cumene was shown in Fig. 1D and E. It can be seen from Fig. 1D that the initial reaction rate was rather slow under 343 K and 353 K, indicating an induction period of 1–2 h. After 2 h, the conversion of cumene rapidly increased with the reaction time. When the reaction temperature reached 373 K, the induction period of oxidation reaction was not apparent. Under the proper reaction temperature of 353 K, the effect of reaction time on the conversion and product distributions was further shown in Fig. 1E. From 2 h to 12 h, the conversion of cumene increased nearly linearly with the reaction time increasing. However, with the accumulation of CHP, its decomposition accelerated, resulting in a low selectivity to CHP. These results reveal that 8 h is a suitable reaction time, with a CHP selectivity of 88.4%.

As shown above, there is a common trade-off relationship between cumene conversion and CHP selectivity. Under the optimal conditions, we can obtain 24.1% conversion of cumene and 88.4% selectivity to CHP. In industry, the cumene conversion was controlled under 30% to make sure over 90% selectivity to CHP with alkaline additives as catalyst under high temperature and pressure [1]. For comparison, 10% (in weight) NaOH aqueous solution as catalyst was tested under the same reaction conditions (entry 2 of Table 1). The result elucidated that CNTs could afford higher cumene conversion without changing the selectivity to CHP. Moreover, compared with frequently-researched CuO catalyst, higher CHP selectivity was obtained over CNTs (entry 3–4 of Table 1), indicating that metal-free carbon catalyst exhibited comparable cumene conversion and CHP selectivity with metal-based catalyst. Therefore, CNTs show a promising application in liquid oxidation

Table 2
Cumene oxidation with different CNTs[a].

Entry	Catalyst	Substrate	S_{BET} (m^2 g^{-1})	Raman (I_D/I_G)	Conversion (%)	Selectivity (%)
1	Blank	Cumene		–	2.7	99.2
2	CNTs	Cumene	85.3	1.50	24.1	88.4
3	Blank[b]	Cumene		–	3.2	93.9
4	CNTs[b]	Cumene		–	31.4	84.9
5	CNTs[c]	Cumene		–	0.1	–
6	Blank[d]	CHP		–	5.5	
7	CNTs[d]	CHP		–	17.3	
8	CNTs-HNO_3-2 h[d]	CHP		–	10.7	
9	CNTs-HNO_3-0.5 h	Cumene	98.8	1.57	4.3	93.0
10	CNTs-HNO_3-2 h	Cumene	104.2	1.71	1.2	91.1
11	CNTs-HNO_3-4 h	Cumene	116.0	1.75	0.8	90.2
12	CNTs-HNO_3-2h-873	Cumene	122.3	1.62	13.1	88.0
13	CNTs-HNO_3-2h-1173	Cumene	141.5	1.54	21.6	86.0

[a] Reaction conditions: cumene 10 mL, catalyst 0.1 g, 353 K, 8 h, O_2 flow rate of 10 cm^3/min.
[b] The addition of 2% CHP.
[c] The addition of *p*-benzoquinone as radical scavenger.
[d] Reaction conditions: CHP 2 g, catalyst 0.1 g, 8 mL acetonitrile as solvent, 353 K, 4 h; the conversion means the decomposition ratio of CHP.

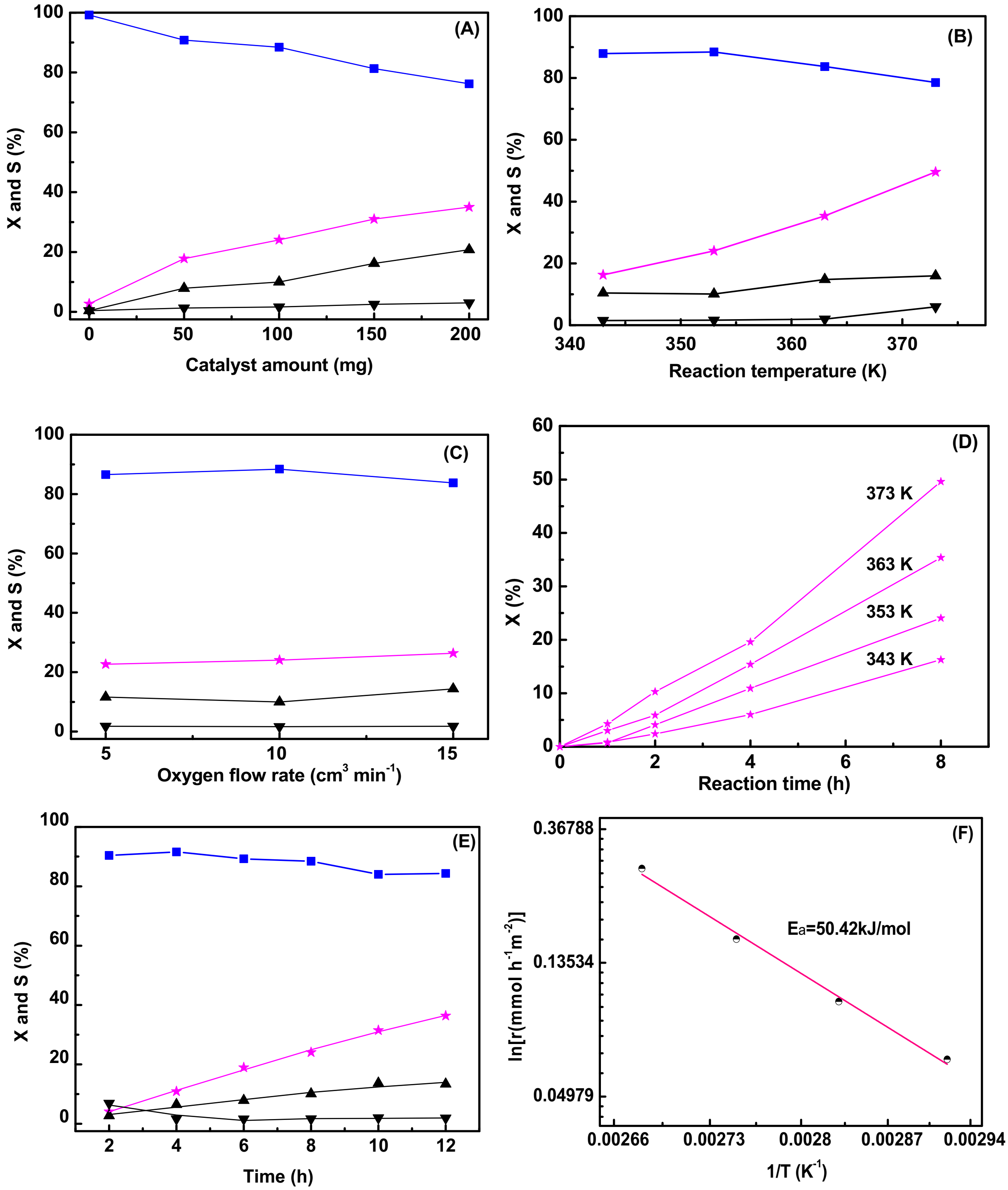

Fig. 1. (A) Effect of catalyst amount on cumene oxidation under 353 K for 8 h. (B) Effect of reaction temperature on cumene oxidation under 100 mg CNTs for 8 h. (C) Effect of O_2 flow rate on the catalytic activity of cumene with O_2 under 100 mg CNTs for 8 h. (D) Effect of reaction time on cumene oxidation under 100 mg CNTs and different temperature. (E) Effect of reaction time on cumene oxidation under 100 mg CNTs and 353 K. (F) The apparent activation energy of cumene oxidation to CHP on CNTs catalyst. Reaction conditions: cumene (10 mL), O_2 flow rate (10 cm^3/min). Cumene conversion (★), CHP selectivity (■), BP selectivity (▲), AP selectivity (▼).

of cumene to CHP due to the low reaction temperature and simple separation process.

3.2. *The catalytic role of carbon catalyst*

It was widely accepted that cumene autoxidation underwent a radical-involved reaction mechanism, involving the initiation of the free-radicals, the chain propagation and transfer and radical termination [3,27,28]. To prove the dominant role of radical species in our system, *p*-benzoquinone as a typical radical scavenger and CHP as a free-radical initiator were added to the reactant (shown in entry 1–5 of Table 2). After adding *p*-benzoquinone, the reaction was nearly totally prevented. With CNTs as catalyst, the conversion increased from 24.1% to 31.4% after the addition of CHP. These indicated that cumene oxidation catalyzed by CNTs is a radical-involved reaction, also proved by the low initial reaction rate under 343 K

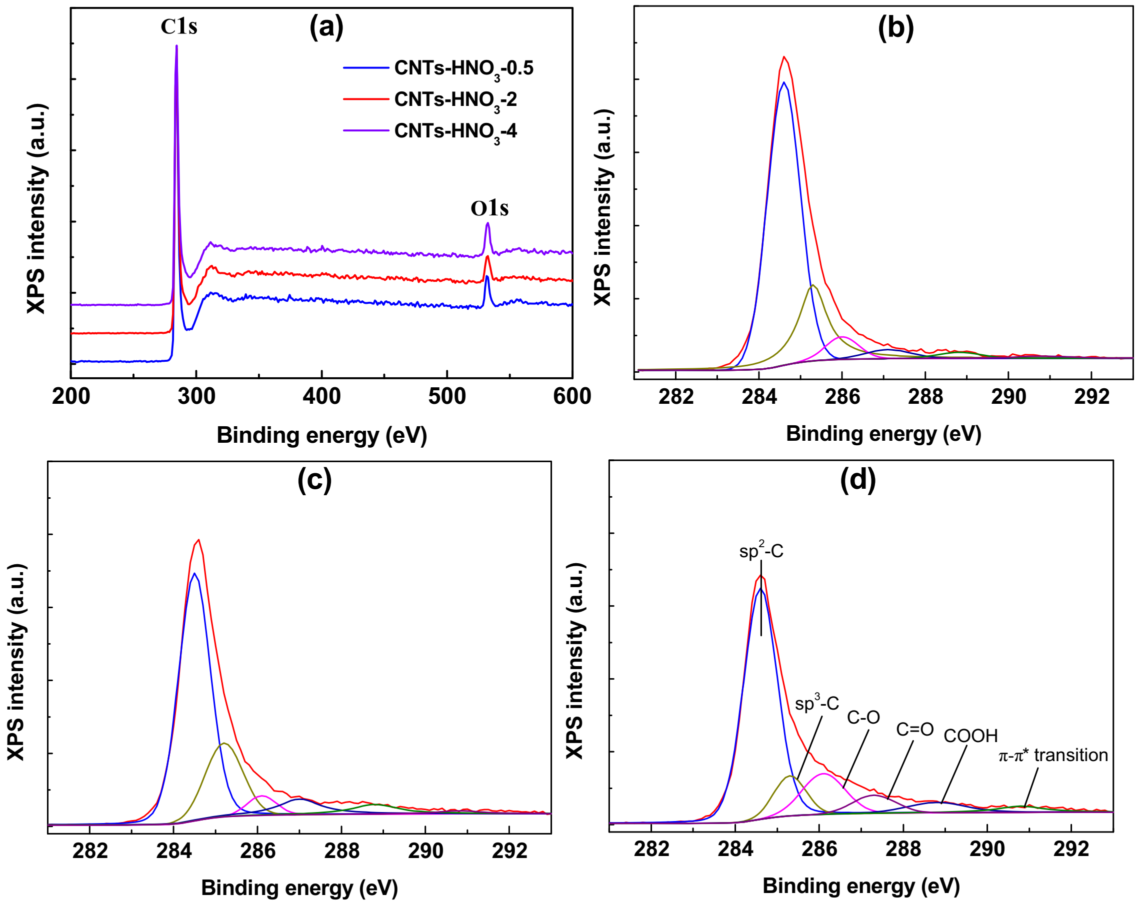

Fig. 2. XPS spectra of different CNTs (a) and deconvolution of XPS C1s spectra of CNTs-HNO$_3$-0.5 (b), CNTs-HNO$_3$-2 (c) and CNTs-HNO$_3$-4 (d).

and 353 K as no initiator (CHP) is added. For blank tests, whether the addition of CHP or not, the conversion of cumene remained very low, possibly because CHP was stable under 353 K. It can be emphasized that both CNTs and CHP play a crucial role in cumene oxidation reaction.

Especially, it was generally agreed that the chain initiation process involved CHP decomposition to produce cumenyl oxygen radical (RO$^\bullet$) which could further abstract hydrogen atom from cumene (RH) to produce cumenyl radical (R$^\bullet$). We also investigated the effect of CNTs on decomposition rate of CHP. As shown in entry 7 of Table 2, CHP decomposition rate on CNTs was about 3.1 times of that in blank example and decomposition products were AP and BP. This offers the preliminary evidence that the good catalytic activity of CNTs in cumene oxidation is attributed to its appropriate decomposition role on CHP. The similar decomposition role of carbon nanotubes on organic peroxides was also reported in Ref. [26], and explained by electron-transfer-introduced decomposition. Actually, the catalytic activity of transition metal catalysts is also related to their appropriate CHP decomposition ability, which is caused by their variable and stable valence [3]. In addition, by controlling the conversion of cumene in nearly 10%, we obtained the apparent activation energy of 50.42 kJ/mol on CNTs as shown in Fig. 1F, which is close to that of 47.72 kJ/mol of metalloporphyrins catalyst [7] and much lower than that of non-catalyzed reaction (71.18 kJ/mol in reference [29]). Hence, CNTs possess some special property similar to transition metals which can greatly decrease the activation energy of cumene oxidation and accelerate the decomposition of CHP.

In previous study, quinone-type oxygen or carboxylic acid functional groups on the surface of CNTs had been thought to be responsible for their excellent catalytic performance [11,15,17]. Hence, it is necessary to discuss the role of oxygenated functional groups in cumene liquid reaction. Oxygenated functional groups were firstly introduced on the surface of carbon nanotubes through

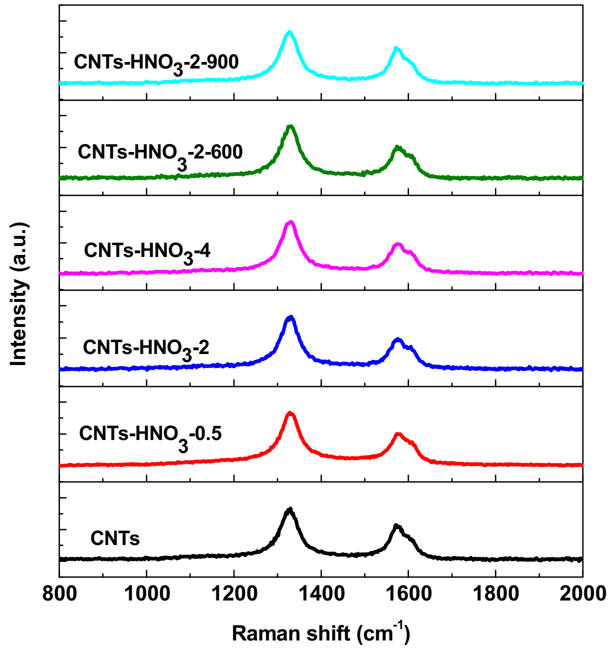

Fig. 3. Raman spectra of the catalysts.

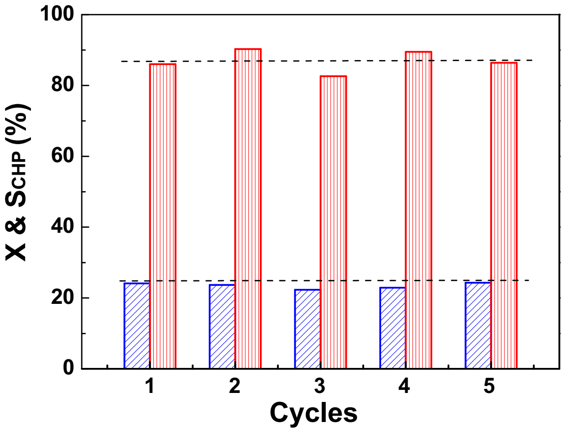

Fig. 4. The reusability of the CNTs for the oxidation of cumene. Reaction conditions: CNTs (100 mg), cumene (10 mL), O_2 flow rate (10 cm^3/min), 353 K, 8 h.

nitric acid oxidation method and then removed by annealing treatment under high temperature. As shown by the XPS data in Fig. 2 and Table 3, the oxygen groups were effectively introduced on the surface of CNTs, and the content increased with prolonged oxidation time. Six components can be deconvoluted from C1s XPS spectra, namely sp^2-hybryidized graphite-like carbon atoms at 284.6 ± 0.1 eV, sp^3-hybryidized carbon atoms at 285.3 eV, C–O–species at 286.1 ± 0.1 eV, $\rangle C{=}O$ species at 287.5 eV, –COOH species at 288.9 eV and π–π^* transition at 290.8 eV, respectively [30]. The intensity ratio (I_D/I_G) of D-band (I_D) to G-band (I_G) in Raman spectrum was used to evaluate the defectiveness of CNTs. The Raman spectra in Fig. 3 indicated that the defect degree increased with oxidation time increasing. However, as shown in entry 9–11 of Table 2, there was a negative effect of oxygen functional groups on cumene oxidation that cumene conversion decreased dramatically after oxidation treatment and further decreased with oxidation time increasing. This result is probably caused by the localization of electrons after the introducing of defects and oxygenated functional groups, which is not favorable for forming π–π interactions between the peroxide and the graphene sheets of oxidized CNTs [19], confirmed by the decreased CHP decomposition rate of CNTs-HNO_3-2 h (entry 8 of Table 2). However, the essential effect of various oxygen forms on the surface of CNTs on catalytic activity remains not clearly distinguishable. The annealing treatment of CNTs can decompose the surface oxygenated groups and repair the defects, indicated by the decrease of I_D/I_G ratios with the increase of annealing temperature. After annealing treatment, the activity of CNTs recovered (entry 12–13 of Table 2), further indicating oxygenated groups and defects are disadvantageous to cumene oxidation. The similar phenomenon was also found in liquid-phase aerobic oxidation of cyclohexane, ethylbenzene, and benzyl alcohol [19,20,31]. Hence, the delocalized π electronic system of CNTs may be preferred for cumene oxidation.

According to above results, it is indicated that the special structure of CNTs contributed to its catalytic performance in cumene oxidation. Many studies also reported that CNTs could activate molecule oxygen based on theoretical calculations [32,33]. Therefore, this reaction process can be interpreted as following. At the initiated stage, oxygen interacts with CNTs to form CNTs$\cdots O_2$ complex, and then the complex continues reacting with RH (cumene) to abstract the H atom to form $R^\bullet$ radical with a low reaction rate as in step (1) and (2). Next, the chain propagation process starts and CHP (ROOH) is formed as described in step (5) and (6). Hence the initial reaction rate is rather low, especially under low temperature of 343 K and 353 K. Once CHP is formed, another chain initiation path also occurs. CHP decomposes to form $RO^\bullet$ radical which can

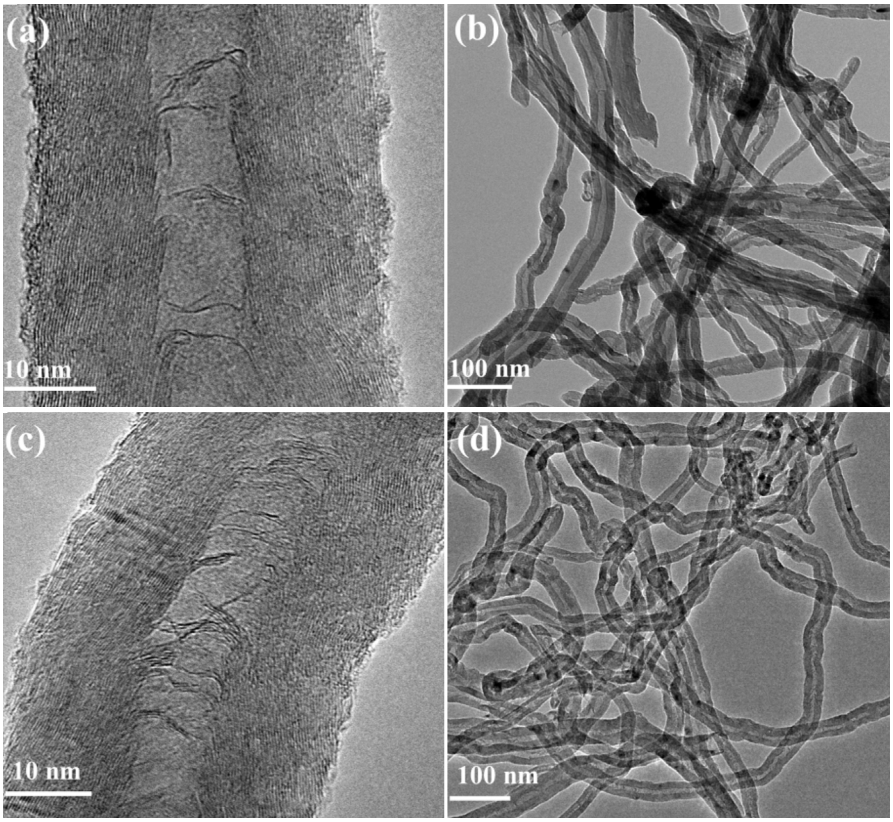

Fig. 5. TEM images of pristine CNTs (a and b) and CNTs after oxidation reaction (c and d).

Table 3
The XPS analysis data of different CNTs.

Catalyst	O (at.%)	C (at.%)	sp^2-C (%)	sp^3-C (%)	C–O (%)	C=O (%)	COOH (%)	π–π^* (%)
CNTs-HNO_3-0.5	2.96	97.04	66.3	22.7	5.3	2.9	1.8	0.9
CNTs-HNO_3-2	3.22	96.78	61.6	20.5	4.3	7.3	4.9	1.4
CNTs-HNO_3-4	5.73	94.27	62.6	9.8	13.3	5.9	5.2	3.2

further react with RH to form R• radical due to the catalytic decomposition role of CNTs, as shown in step (3) and (4). At the same time, by-product BP (ROH) is produced. It need be emphasized that the decomposition of CHP on CNTs is not so quick that a high CHP selectivity can be obtained. However, this decomposition role is effective to produce R• radical, and the chain propagation reactions of (5) and (6) are enhanced, more and more CHP is formed, resulting in the rapidly increased conversion of cumene. Another by-product $(C_6H_5)COCH_3$ (AP) is produced through the β-scission of RO• in step (7), which also depends on the catalytic decomposition role of CNTs (3).

Chain initiation:

$$\mathrm{CNTs} + O_2 \rightarrow \mathrm{CNTs}\cdots O_2 \qquad (1)$$

$$\mathrm{CNTs}\cdots O_2 + \mathrm{RH} \rightarrow \mathrm{CNTs}\cdots \mathrm{OOH} + \mathrm{R}^{\bullet} \qquad (2)$$

$$\mathrm{ROOH} \xrightarrow{\mathrm{CNTs}} \mathrm{RO}^{\bullet} + \mathrm{HO}^{\bullet} \qquad (3)$$

$$\mathrm{RO}^{\bullet} + \mathrm{RH} \rightarrow \mathrm{ROH} + \mathrm{R}^{\bullet} \qquad (4)$$

Chain propagation:

$$\mathrm{R}^{\bullet} + O_2 \rightarrow \mathrm{ROO}^{\bullet} \qquad (5)$$

$$\mathrm{ROO}^{\bullet} + \mathrm{RH} \rightarrow \mathrm{ROOH} + \mathrm{R}^{\bullet} \qquad (6)$$

$$\mathrm{RO}^{\bullet} \rightarrow (C_6C_5)COCH_3 + CH_3^{\bullet} \qquad (7)$$

3.3. The stability of carbon catalyst

In addition to the remarkable catalytic performance, the recyclability of the catalyst was also studied as shown in Fig. 4. After every run, the recycled catalyst was repeatedly washed by deionized water and ethanol. During five cycling tests, no obvious decrease in both cumene conversion and CHP selectivity was found, indicating that CNTs catalyst shows outstanding recyclability. Moreover, as shown in Fig. 5, compared with the pristine CNTs, it was observed that the morphology of the used CNTs kept stable and unchanged obviously. It indicates that CNTs are stable during the conversion of cumene and formation of CHP, and show excellent potential for industrial application of cumenen oxidation to cumene hydroperoxide.

4. Conclusions

In this work, we reported that the commercial CNTs could be used as effective catalyst for the liquid aerobic oxidation of cumene to CHP under low temperature. After the optimization of reaction conditions, an excellent cumene conversion of 24.1% with CHP selectivity to 88.4% was obtained. Cumene oxidation catalyzed by CNTs was proved a radical-involved reaction, and the outstanding catalytic performance was attributed to CHP decomposition catalyzed by CNTs. Oxygenated functional groups on the surface of catalyst showed a negative effect on cumene oxidation due to the localization of electrons after the introducing of defects and oxygenated functional groups. In addition, CNTs also showed good recyclability during the conversion of cumene and formation of peroxide, and exhibited excellent potential for industrial application of cumenen oxidation to CHP. This study not only provides an applicable method for selective oxidation of cumene to CHP, but also gives some useful information on catalytic role of CNT-catalyzed liquid oxidation reactions of aromatic hydrocarbons.

Acknowledgments

This work was supported by the National Natural Science Foundation of China (Nos. 21133010, 21273079), the Guangdong Provincial Natural Science Foundation (No. S20120011275), Program for New Century Excellent Talents in Universities of China (NCET-12-0190), and Jiangsu Provincial Science and Technology Project (BE2012127).

References

[1] A.K. Suresh, M.M. Sharma, T. Sridhar, Engineering aspects of industrial liquid-phase air oxidation of hydrocarbons, Ind. Eng. Chem. Res. 39 (2000) 3958–3997.
[2] S. Matsui, T. Fujita, New cumene-oxidation systems: O_2 activator effects and radical stabilizer effects, Catal. Today 71 (2001) 145–152.
[3] Y.F. Hsu, C.P. Cheng, Mechanistic investigation of the autooxidation of cumene catalyzed by transition metal salts supported on polymer, J. Mol. Catal. A: Chem. 136 (1998) 1–11.
[4] M. Zhang, L. Wang, H. Ji, B. Wu, X. Zeng, Cumene liquid oxidation to cumene hydroperoxide over CuO nanoparticle with molecular oxygen under mild condition, J. Nat. Gas Chem. 16 (2007) 393–398.
[5] S. Xu, C. Huang, J. Zhang, B. Chen, Catalytic activity of Cu/MgO in liquid phase oxidation of cumene, Korean J. Chem. Eng. 26 (2009) 1568–1573.
[6] R.M. Wang, E.X. Hao, G.R. Shen, Y.F. He, Z.Q. Lei, Polymeric Salphen-phthalocyanine dinuclear metal complexes for activation of molecular oxygen, J. Appl. Polym. Sci. 111 (2009) 1999–2005.
[7] W.J. Yang, C.C. Guo, N.Y. Tao, J. Cao, Aerobic oxidation of cumene to cumene hydroperoxide catalyzed by metalloporphyrins, Kinet. Catal. 51 (2010) 194–199.
[8] Y.F. Hsu, C.P. Cheng, Polymer supported catalyst for the effective autoxidation of cumene to cumene hydroperoxide, J. Mol. Catal. A: Chem. 120 (1997) 109–116.
[9] J. Planeix, N. Coustel, B. Coq, V. Brotons, P. Kumbhar, R. Dutartre, P. Geneste, P. Bernier, P. Ajayan, Application of carbon nanotubes as supports in heterogeneous catalysis, J. Am. Chem. Soc. 116 (1994) 7935–7936.
[10] P. Serp, E. Castillejos, Catalysis in carbon nanotubes, ChemCatChem 2 (2010) 41–47.
[11] D.S. Su, J. Zhang, B. Frank, A. Thomas, X. Wang, J. Paraknowitsch, R. Schlogl, Metal-free heterogeneous catalysis for sustainable chemistry, ChemSusChem 3 (2010) 169–180.
[12] D. Su, N.I. Maksimova, G. Mestl, V.L. Kuznetsov, V. Keller, R. Schlogl, N. Keller, Oxidative dehydrogenation of ethylbenzene to styrene over ultra-dispersed diamond and onion-like carbon, Carbon 45 (2007) 2145–2151.
[13] X. Liu, D.S. Su, R. Schlogl, Oxidative dehydrogenation of 1-butene to butadiene over carbon nanotube catalysts, Carbon 46 (2008) 547–549.
[14] J. Zhang, X. Liu, R. Blume, A. Zhang, R. Schlogl, D.S. Su, Surface-modified carbon nanotubes catalyze oxidative dehydrogenation of n-butane, Science 322 (2008) 73–77.
[15] S. Yang, X. Li, W. Zhu, J. Wang, C. Descorme, Catalytic activity, stability and structure of multi-walled carbon nanotubes in the wet air oxidation of phenol, Carbon 46 (2008) 445–452.
[16] C. Aguilar, R. García, G. Soto-Garrido, R. Arriagada, Catalytic wet air oxidation of aqueous ammonia with activated carbon, Appl. Catal. B: Environ. 46 (2003) 229–237.
[17] R.P. Rocha, J.P. Sousa, A.M. Silva, M.F. Pereira, J.L. Figueiredo, Catalytic activity and stability of multiwalled carbon nanotubes in catalytic wet air oxidation of oxalic acid: the role of the basic nature induced by the surface chemistry, Appl. Catal. B: Environ. 104 (2011) 330–336.
[18] B. Frank, R. Blume, A. Rinaldi, A. Trunschke, R. Schlogl, Oxygen insertion catalysis by sp2 carbon, Angew. Chem. Int. Ed. 50 (2011) 10226–10230.
[19] H. Yu, F. Peng, J. Tan, X. Hu, H. Wang, J. Yang, W. Zheng, Selective catalysis of the aerobic oxidation of cyclohexane in the liquid phase by carbon nanotubes, Angew. Chem. Int. Ed. 50 (2011) 3978–3982.
[20] J. Luo, F. Peng, H. Yu, H. Wang, W. Zheng, Aerobic liquid-phase oxidation of ethylbenzene to acetophenone catalyzed by carbon nanotubes, ChemCatChem 5 (2013) 1578–1586.
[21] J.H. Yang, G. Sun, Y. Gao, H. Zhao, P. Tang, J. Tan, A.H. Lu, D. Ma, Direct catalytic oxidation of benzene to phenol over metal-free graphene-based catalyst, Energ. Environ. Sci. 6 (2013) 793–798.

[22] A. Rinaldi, J. Zhang, B. Frank, D.S. Su, S.B. Abd Hamid, R. Schlogl, Oxidative purification of carbon nanotubes and its impact on catalytic performance in oxidative dehydrogenation reactions, ChemSusChem 3 (2010) 254–260.

[23] B. Frank, A. Rinaldi, R. Blume, R. Schlogl, D.S. Su, Oxidation stability of multiwalled carbon nanotubes for catalytic applications, Chem. Mater. 22 (2010) 4462–4470.

[24] J. Zawadiak, D. Gilner, Z. Kulicki, S. Baj, Concurrent iodimetric determination of cumene hydroperoxide and dicumenyl peroxide used for reaction control in dicumenyl peroxide synthesis, Analyst 118 (1993) 1081–1083.

[25] V.Y. Kugel, M. Tsodikov, G. Bondarenko, Y.V. Slivinskii, D. Kochubey, M. Hidalgo, J. Navio, Study of the initiation route of cumene liquid-phase oxidation over iron-aluminum oxide catalysts obtained by the alkoxy method, Langmuir 15 (1999) 463–468.

[26] P.S. Engel, W.E. Billups, D.W. Abmayr, K. Tsvaygboym, R. Wang, Reaction of single-walled carbon nanotubes with organic peroxides, J. Phys. Chem. C 112 (2008) 695–700.

[27] A. Bhattacharya, Kinetic modeling of liquid phase autoxidation of cumene, Chem. Eng. J. 137 (2008) 308–319.

[28] B. Orlińska, N-Hydroxyphthalimide in combination with Cu (II), Co (II) or Mn (II) salts as catalytic systems for the oxidation of isopropyl-aromatic hydrocarbons with oxygen, Tetrahedron Lett. 51 (2010) 4100–4102.

[29] J. Casemier, B. Nieuwenhuys, W. Sachtler, The oxidation of cumene and the decomposition of cumene hydroperoxide on silver, copper, and platinum, J. Catal. 29 (1973) 367–373.

[30] H. Ago, T. Kugler, F. Cacialli, W.R. Salaneck, M.S. Shaffer, A.H. Windle, R.H. Friend, Work functions and surface functional groups of multiwall carbon nanotubes, J. Phys. Chem. B 103 (1999) 8116–8121.

[31] J. Luo, F. Peng, H. Yu, H. Wang, Selective liquid phase oxidation of benzyl alcohol catalyzed by carbon nanotubes, Chem. Eng. J. 204–206 (2012) 98–106.

[32] F. Atamny, J. Blöcker, A. Dübotzky, H. Kurt, O. Timpe, G. Loose, W. Mahdi, R. Schlögl, Surface chemistry of carbon: activation of molecular oxygen, Mol. Phys. 76 (1992) 851–886.

[33] R. Khorrampour, M.D. Esrafili, N.L. Hadipour, Density functional theory study of atomic oxygen, O_2 and O_3 adsorptions on the H-capped (5, 0) single-walled carbon nanotube, Physica E 41 (2009) 1373–1378.